A New Class of Color Filter Arrays with Optimal Sensing Properties

Laurent Condat

A New Class of Color Filter Arrays with Optimal Sensing Properties

Laurent Condat

GREYC Lab., Image Team, Caen, France
laurent.condat@greyc.ensicaen.fr

***Abstract*— Digital color cameras acquire color images by means of a sensor on which a color filter array (CFA) is overlaid. The Bayer CFA dominates the consumer market and little attention has been directed to the design of alternative CFAs in the literature. Recent works of Hirakawa *et al.* [1]–[4] introduced new insights in this field by focusing on the spectral properties of CFAs and operating directly in the Fourier domain. However, this new paradigm is generic and leaves open questions about the optimization of the many available parameters. In this work, we investigate the link between them and the light sensitivity and color discrimination capabilities of the CFA. Indeed, these characteristics determine the quality of the whole imaging pipeline, since they directly control its sensitivity to noise. By optimizing the key parameters, we obtain a class of new CFAs with optimal properties, in which the shortest 2×3 pattern shows up as the best compromise. Moreover, a simple and efficient linear demosaicking algorithm is associated to these CFAs, which fully exploits their spectral properties. Practical experiments confirm the superiority of our new design.**

***Index Terms*— Color filter array (CFA), color imaging, demosaicking, digital camera pipeline, spatio-spectral sampling, luminance/chrominance gains, noise sensitivity.**

I. Introduction

The growing popularity of digital photography demands every attempt of improvement in terms of quality and speed of the features provided in digital cameras. The heart of a digital still or video camera is its sensor, a 2-D array of light-sensitive diodes (photosites) that measure the amount of light absorbed during the exposure time. Since only one measurement is performed by each photosite, the color information is obtained by means of a *color filter array* (CFA) overlaid on the sensor, such that each photosite is covered by a color filter sensitive to only a portion of the visible light spectrum [5]. For a sensor with given geometry, the CFA is the most crucial element in the imaging pipeline that determines the image quality [5], [6]. From the *mosaicked image* acquired by the camera, some processing is required to recover a full color image with three components per pixel, carrying information in the red (R), green (G) and blue (B) spectral bands to which the human visual system (HVS) is sensitive. This reconstruction operation is called *demosaicking*, see e.g. [5], [7]–[9].

This work was performed in part during the stay of the author at the Helmholtz Zentrum München — German Research Center for Environmental Health, Neuherberg, Germany, where he was supported by the Marie Curie Excellence Team Grant MEXT-CT-2004-013477, Acronym MAMEBIA, funded by the European Commission.

The Bayer CFA [10], which consists in filters with the primary colors R,G,B, is the most popular and dominates the consumer market. Other CFAs have been proposed and are currently used in some imaging devices; some of these are compared in [11]. We can mention for instance the CMY CFA, where the R,G,B filters of the Bayer CFA are replaced by filters with the complementary colors C (cyan), M (magenta) and Y (yellow), yielding a doubled sensitivity. Also, Kodak recently patented new CFAs containing transparent (panchromatic) filters, in addition to R,G,B filters [12]. They should replace the Bayer CFA in the next generation of cameras of this manufacturer. However, all these CFAs (see also [7], [13]–[15]) have been designed empirically, and a thorough theory for CFA design has been lacking so far. There is a vast literature dealing with the best way to reduce artifacts during the demosaicking process, but these artifacts inherently originate from the suboptimal choice of the Bayer CFA itself.

A breakthrough in the field was made recently by Hirakawa *et al.*, who proposed to design CFAs directly in the Fourier domain, without constraints on the colors of the filters in the spatial domain. Based on previous work characterizing the spectral properties of the Bayer CFA [8] and showing that the mosaicked image actually consists in the superposition of modulated signals encoding the color information, they proposed to design a CFA so that these signals, expressed in some basis where they are decorrelated, tile the frequency plane with minimum overlap [1]–[3]. However, this paradigm is quite general and it leaves open questions about the choice of the many degrees of freedom that are left free.

The aim of this work is to investigate the link between these parameters and the *light sensitivity* and *color discrimination capabilities* of the CFA, hence, its sensitivity to noise, which is crucial for the quality of the whole imaging pipeline. In fact, the mosaicked image, which encodes the three channels of the color scene together, is corrupted by noise in practice [16]. Thus, the image quality after subsequent reconstruction (demosaicking) directly depends on the signal-to-noise ratio for each of the three channels. Moreover, higher sensitivity properties allow, when acquiring a given picture, to reduce the exposure time (for less blur due to shake of the camera) or to increase the aperture (for increased depth-of-field, hence less out-of-focus blur). This is particularly important for photography in low-light level environments. Hence, the need really exists for developing new CFAs with improved light sensitivity. So, the essence of CFA design consists in ensuring

that *maximum energy of the color scene is packed into the mosaicked image*. However, the sensitivity of a CFA with respect to the luminance and the one with respect to the chrominance information (the ability to discriminate colors) are antagonist characteristics. For instance, a transparent CFA lets all the photons reach the sensor, and then has maximum light sensitivity, but the color information is completely lost.

In this work, by optimizing the key parameters in the Fourier domain, we show how to design CFAs that attain the best possible compromise in this respect, while at the same time being little prone to inter-channel aliasing. The paper is organized as follows. In Section II, we express the design problem in the Fourier domain, using a characterization of the spectral properties of CFAs in an appropriate luminance/chrominance basis that decorrelates the degrees of freedom. In Section III, we put some requirements on the design and tune the remaining parameters to obtain a class of new CFAs with optimal sensitivity properties and robustness to inter-channel aliasing. We then discuss in Section IV the criteria of choice that play an important role when choosing a particular CFA in this class. As a result, the CFA with 2×3 periodicity appears as a well-balanced compromise with many advantages over every other design for high image fidelity. In Section V, we present a simple and efficient linear demosaicking method that fully exploits the specificities of our new CFAs. We illustrate in Section VI the relevance of the proposed design by practical experiments, which show its superiority both in noiseless and noisy situations.

II. Spectral Characterization of CFAs

In this article, boldface quantities denote vectors, e.g. $\mathbf{k} = [k_1, k_2]^{\mathrm{T}} \in \mathbb{Z}^2$ and $\mathbf{0} = [0, 0]^{\mathrm{T}}$.

We define a CFA as a color image $\mathbf{cfa} = (\mathbf{cfa}[\mathbf{k}])_{\mathbf{k}\in\mathbb{Z}^2}$, where $\mathbf{cfa}[\mathbf{k}] = \left[\mathrm{cfa}^R[\mathbf{k}], \mathrm{cfa}^G[\mathbf{k}], \mathrm{cfa}^B[\mathbf{k}]\right]^{\mathrm{T}} \in [0,1]^3$ is the color value in the R,G,B basis of the filter centered at the location $\mathbf{k}$. For instance, a green filter corresponds to $[0,1,0]^{\mathrm{T}}$. We put emphasis on the fact that the components of $\mathbf{cfa}[\mathbf{k}]$ are constrained to lie in $[0,1]$ for physical realizability. Also, the color values correspond to opacity rates: the white color $[1,1,1]^{\mathrm{T}}$ stands for a transparent filter. A CFA $\mathbf{cfa}$ is periodic with generating pattern of size $N_1 \times N_2$ if $\mathbf{cfa}[k_1 + N_1, k_2] = \mathbf{cfa}[k_1, k_2 + N_2] = \mathbf{cfa}[\mathbf{k}]$ for every $\mathbf{k}$. We focus in this work on periodic CFAs; thus, the design of CFAs having a random pattern, like e.g. in [15], is beyond the scope of this paper. Also, we consider patterns defined on the square lattice, but the principles developed in this work could be extended to other geometries, e.g. hexagonal arrangements.

We define the color image $\mathbf{im} = (\mathbf{im}[\mathbf{k}])_{\mathbf{k}\in\mathbb{Z}^2}$ as the ground truth to be estimated by the demosaicking process. That is, $\mathbf{im}[\mathbf{k}]$ is the vector of the three R,G,B values that would have been obtained by the photosite at the location $\mathbf{k}$, if three measurements had been performed using R,G,B filters in front of the sensor. Consequently, the mosaicked image $v = (v[\mathbf{k}])_{\mathbf{k}\in\mathbb{Z}^2}$ is such that

$$v[\mathbf{k}] = \mathbf{im}[\mathbf{k}]^{\mathrm{T}}\mathbf{cfa}[\mathbf{k}] \qquad \forall \mathbf{k} \in \mathbb{Z}^2. \tag{1}$$

Note that this model holds in the ideal noise free situation. In practice, an additive random term modeling the effect of noise has to be added in (1) [16].

It is well known that in natural images, the R,G,B components are not independent [5], [17]–[20]. Thus, we define the orthonormal basis corresponding to luminance, red/green and yellow/blue chrominance, as

$$L = \frac{1}{\sqrt{3}}[1,1,1]^{\mathrm{T}}, C_1 = \frac{1}{\sqrt{2}}[-1,1,0]^{\mathrm{T}}, C_2 = \frac{1}{\sqrt{6}}[-1,-1,2]. \tag{2}$$

We denote u^L, u^{C_1}, and u^{C_2} the components of a color signal $\mathbf{u}$ in this basis. According to the theory of opponent colors, validated by experimental evidences [21], this luminance/chrominance basis is a good model of the three channels used in the HVS to process the visual information. In fact, the components of natural images can be considered as statistically independent in this basis [17].

There is a temptation to define the luminance with a higher weight for the green channel, arguing that the contrast sensitivity function of the HVS is higher for this channel. For this reason, the Bayer CFA has twice more green filters as red or blue ones. However, contrary to what Bayer thought as he designed his CFA, having more green filters does not enable a better estimation of the luminance, as shown in [8]. Actually, exchanging the blue and green colors in the Bayer pattern can improve the quality of the demosaicking process [8]. So, we prefer defining the luminance without preferred color component. This ensures the orthogonality of the L, C_1, C_2 basis for maximum decorrelation of the image content in this basis.

In order to analyse the properties of the Bayer CFA, Alleysson *et al.* showed that the mosaicked image v can be interpreted, in the Fourier domain, as the sum of the luminance and chrominance components of the color reference image $\mathbf{im}$, moved at different locations of the frequency plane [8]. We extend this characterization to every CFA, by simply writing $\mathbf{cfa}$ as the sum of its Fourier components:

$$\mathrm{cfa}^X[\mathbf{k}] = \sum_{n_1=\lfloor\frac{N_1-1}{2}\rfloor}^{\lfloor\frac{N_1}{2}\rfloor} \sum_{n_2=0}^{\lfloor\frac{N_2}{2}\rfloor} \alpha_{\mathbf{n}}^X \cos\left(\frac{2\pi n_1}{N_1}k_1 + \frac{2\pi n_2}{N_2}k_2\right) + \beta_{\mathbf{n}}^X \sin\left(\frac{2\pi n_1}{N_1}k_1 + \frac{2\pi n_2}{N_2}k_2\right) \tag{3}$$

for every $X \in \{L, C_1, C_2\}$ and $\mathbf{k} \in \mathbb{Z}^2$, where $\lfloor\cdot\rfloor$ is the rounding operator to the nearest smaller integer. So, the design of $\mathbf{cfa}$ turns out to choosing its $3N_1N_2$ Fourier coefficients $\alpha_{\mathbf{n}}^X$ and $\beta_{\mathbf{n}}^X$ appropriately. For this, we express the Fourier transform $\hat{v}(\boldsymbol{\omega}) = \sum_{\mathbf{k}\in\mathbb{Z}^2} v[\mathbf{k}]e^{-j\boldsymbol{\omega}^{\mathrm{T}}\mathbf{k}}$ in function of the Fourier transforms of the components of $\mathbf{im}$:

$$\hat{v}(\boldsymbol{\omega}) = \sum_{X\in\{L,C_1,C_2\}} \sum_{n_1=\lfloor\frac{N_1-1}{2}\rfloor}^{\lfloor\frac{N_1}{2}\rfloor} \sum_{n_2=0}^{\lfloor\frac{N_2}{2}\rfloor} \frac{\alpha_{\mathbf{n}}^X}{2}\left(\widehat{\mathrm{im}^X}\left(\boldsymbol{\omega} + \left[\tfrac{2\pi n_1}{N_1}, \tfrac{2\pi n_2}{N_2}\right]^{\mathrm{T}}\right) + \widehat{\mathrm{im}^X}\left(\boldsymbol{\omega} - \left[\tfrac{2\pi n_1}{N_1}, \tfrac{2\pi n_2}{N_2}\right]^{\mathrm{T}}\right)\right) + \frac{\beta_{\mathbf{n}}^X}{2j}\left(\widehat{\mathrm{im}^X}\left(\boldsymbol{\omega} + \left[\tfrac{2\pi n_1}{N_1}, \tfrac{2\pi n_2}{N_2}\right]^{\mathrm{T}}\right) - \widehat{\mathrm{im}^X}\left(\boldsymbol{\omega} - \left[\tfrac{2\pi n_1}{N_1}, \tfrac{2\pi n_2}{N_2}\right]^{\mathrm{T}}\right)\right) \tag{4}$$

for every $\boldsymbol{\omega} \in \mathbb{R}^2$. So, for every CFA, we can write the Fourier transform of the mosaicked image as the sum of the luminance and chrominance components $\widehat{\mathrm{im}^X}$, replicated at the sites of the dual lattice induced by the periodicity of the pattern.

In the spatial domain, this corresponds to writing v as the sum of the luminance and chrominance channels of $\mathbf{im}$, each one being modulated by some specific carrier wave: expanding (1) in the L, C_1, C_2 basis, we get

$$v[\mathbf{k}] = \sum_{X \in \{L, C_1, C_2\}} \mathrm{im}^X[\mathbf{k}] \times \sum_{n_1 = \lfloor \frac{N_1 - 1}{2} \rfloor}^{\lfloor \frac{N_1}{2} \rfloor} \sum_{n_2 = 0}^{\lfloor \frac{N_2}{2} \rfloor} \alpha_{\mathbf{n}}^X \cos\left(\frac{2\pi n_1}{N_1} k_1 + \frac{2\pi n_2}{N_2} k_2\right) + \beta_{\mathbf{n}}^X \sin\left(\frac{2\pi n_1}{N_1} k_1 + \frac{2\pi n_2}{N_2} k_2\right). \quad (5)$$

The major contribution of Hirakawa *et al.* to the problem of CFA design was the idea of directly designing the CFA in the Fourier domain by optimizing the carrier waves, so that the baseband luminance is at the origin and the chrominance is modulated far away from it [1]–[3]. This constrains the degrees of freedom $N_1, N_2, \alpha_{\mathbf{n}}^X, \beta_{\mathbf{n}}^X$ to some extent, but the question of further defining the many remaining parameters is left open. This is the aim of this work to show how tuning these parameters to obtain a CFA with optimal sensitivity characteristics, hence, robustness of the imaging pipeline to sensor noise. We note that Hirakawa *et al.* work with the G, $R - G$, $B - G$ basis, which is not orthogonal and does not decorrelate the color image content at best. Separating the carrier waves in the basis L, C_1, C_2 instead, as done in this work, allows to reduce the bandwidth of the chrominance channels—hence, aliasing with the luminance—even more.

III. A New Family of CFAs with Optimal Sensitivity Characteristics

We now construct step by step a family of CFAs by enforcing some design criteria in the frequency domain. Thus, we progressively reduce the number of degrees of freedom to finally obtain a class of CFAs parameterized by only two values. We discuss the optimization of these remaining parameters in the next section.

The requirements we adopt are the following:

Condition 1) For the CFA to be physically realizable, the values $\mathrm{cfa}^X[\mathbf{k}]$ have to lie in $[0, 1]$. This implies that $\alpha_{\mathbf{0}}^L > 0$. In other words, the luminance of $\mathbf{im}$ appears in the low-frequency part of v. In order to avoid aliasing of the luminance information, we impose that there be no replica of the luminance at other frequencies than zero, in the spectrum of v; that is,

$$\alpha_{\mathbf{n}}^L = \beta_{\mathbf{n}}^L = 0 \qquad \forall \mathbf{n} \neq \mathbf{0}. \quad (6)$$

Also, having a uniform quantum efficiency accross the image plane reduces the issues of under- and over-saturation of the sensor measurements. Hence, (3) gives $\mathrm{cfa}^L[\mathbf{k}] = \alpha_{\mathbf{0}}^L$, which is then a constant. Further on, we rewrite this value $\gamma^L = \alpha_{\mathbf{0}}^L$ and call it the *luminance gain* of the CFA. This value lies in the interval $[0, \sqrt{3}]$ and characterizes the average light sensitivity of the CFA. This is a crucial parameter, as explained in the Introduction. The Bayer CFA satisfies this condition, with $\mathrm{cfa}^R[\mathbf{k}] + \mathrm{cfa}^G[\mathbf{k}] + \mathrm{cfa}^B[\mathbf{k}] = 1$; hence, its luminance gain is $1/\sqrt{3}$.

Condition 2) Since the three luminance and chrominance channels of $\mathbf{im}$ are assumed mutually independent, we impose, in order to be able to separate them optimally during the demosaicking process, that their carrier waves in (5) be orthogonal. This yields the condition

$$\sum_{n_1 = \lfloor \frac{N_1 - 1}{2} \rfloor}^{\lfloor \frac{N_1}{2} \rfloor} \sum_{n_2 = 0}^{\lfloor \frac{N_2}{2} \rfloor} \alpha_{\mathbf{n}}^X \alpha_{\mathbf{n}}^Y + \beta_{\mathbf{n}}^X \beta_{\mathbf{n}}^Y = 0, \quad (7)$$

for every $X, Y \in \{L, C_1, C_2\}$, $X \neq Y$.

As a first consequence, due to the condition 1), we obtain $\alpha_{\mathbf{0}}^{C_1} = \alpha_{\mathbf{0}}^{C_2} = 0$: there is no chrominance in the low-frequency part of v. This also means that the CFA will capture, in average, the same amount of R, G and B light:

$$\sum_{k_1=1}^{N_1} \sum_{k_2=1}^{N_2} \mathrm{cfa}^R[\mathbf{k}] = \sum_{k_1=1}^{N_1} \sum_{k_2=1}^{N_2} \mathrm{cfa}^G[\mathbf{k}] = \sum_{k_1=1}^{N_1} \sum_{k_2=1}^{N_2} \mathrm{cfa}^B[\mathbf{k}]. \quad (8)$$

The Bayer CFA does not satisfy this requirement, with a sensitivity to G two times higher than the one to B or R.

Condition 3) Since the chrominance of $\mathbf{im}$ appears in the high-frequency content of v while the luminance is in the low frequency part, the quality of the demosaicked image is essentially linked to the ability of correctly separating these two parts of v in the frequency domain. In order to maximally reduce the overlaps between the channels, we impose the chrominance to be shifted at only one frequency $\pm\boldsymbol{\omega}_0$. Hence, the information of luminance is concentrated around $\mathbf{0}$ in $\hat{v}$, while the chrominance is around $\pm\boldsymbol{\omega}_0$. So, the expression of the chrominance of $\mathbf{cfa}$ simplifies to

$$\mathrm{cfa}^X[\mathbf{k}] = \alpha^X \cos(\boldsymbol{\omega}_0^{\mathrm{T}} \mathbf{k}) + \beta^X \sin(\boldsymbol{\omega}_0^{\mathrm{T}} \mathbf{k}) \quad \forall X \in \{C_1, C_2\}. \quad (9)$$

The Bayer CFA does not satisfy this condition, with the chrominance spread at the frequencies $[\pi, 0]^{\mathrm{T}}$, $[0, \pi]^{\mathrm{T}}$, $[\pi, \pi]^{\mathrm{T}}$ [8].

Due to the condition 2), the carrier waves for the two chrominance channels are sines in quadrature: $\alpha^{C_1}\alpha^{C_2} + \beta^{C_1}\beta^{C_2} = 0$. So, there is no overlap of the two informations of chrominance, since they occupy the same frequency band, but with different phases. In comparison with designs where the chrominance is spread at several frequencies, like in [2], the risk of inter-chrominance aliasing is drastically reduced, see the example in Fig. 6. Note that this condition excludes the frequencies $[0, \pi]^{\mathrm{T}}$, $[\pi, 0]^{\mathrm{T}}$ and $[\pi, \pi]^{\mathrm{T}}$ as admissible values for $\boldsymbol{\omega}_0$.

Condition 4) We impose that the gain of the two chrominance channels be the same, so that the color discrimination of the CFA is the same for every color, without privileged chrominance axis. That is,

$$(\alpha^{C_1})^2 + (\beta^{C_1})^2 = (\alpha^{C_2})^2 + (\beta^{C_2})^2 = 2(\gamma^C)^2, \quad (10)$$

where we introduce γ^C, the *chrominance gain* of the CFA. Consequently, we can rewrite (9) as

$$\mathrm{cfa}^{C_1}[\mathbf{k}] = \gamma^C \sqrt{2} \cos(\boldsymbol{\omega}_0^{\mathrm{T}} \mathbf{k} - \varphi) \tag{11}$$

$$\mathrm{cfa}^{C_2}[\mathbf{k}] = \gamma^C \sqrt{2} \sin(\boldsymbol{\omega}_0^{\mathrm{T}} \mathbf{k} - \varphi), \tag{12}$$

for every $\mathbf{k} \in \mathbb{Z}^2$, where the phase φ is, at this point, a free degree of freedom.

We can note that the only known CFAs with R,G,B filters satisfying the four previous conditions are the horizontal or vertical or diagonal stripe CFAs, depicted in [11, Fig. 2 d),e)]. Since we do not impose constraints on the colors of the filters, we can find CFAs with much better properties, as will be shown in the following.

Condition 5) For every CFA $\mathbf{cfa}$, we define the *reversed* CFA $\mathcal{R}\mathbf{cfa}$ by $\mathcal{R}\mathrm{cfa}^X[\mathbf{k}] = 1 - \mathrm{cfa}^X[\mathbf{k}]$ for every $X \in \{R, G, B\}, \mathbf{k} \in \mathbb{Z}^2$. $\mathcal{R}\mathbf{cfa}$ has exactly the same chrominance carrier waves (up to a change of sign) as $\mathbf{cfa}$; hence, the same chrominance gain, if defined. Only the luminance gain is changed to $\sqrt{3} - \gamma^L$. For instance, applying this reversal process to the Bayer CFA gives the CMY CFA. Therefore, since the light sensitivity of a CFA is one of its most crucial characteristics, we impose

$$\gamma^L \geq \frac{\sqrt{3}}{2}. \tag{13}$$

That is, given a CFA that does not satisfy this condition, we apply the reversal process to it. This may increase the amount of demosaicking artifacts due to luminance/chrominance aliasing (the ratio γ^C/γ^L is reduced), but this is largely compensated by the increased light sensitivity. Indeed, the improved signal-to-noise ratio for the luminance signal yields a smaller amount of noise in the luminance channel of the demosaicked image.

Condition 6) The farther the chrominance from the zero frequency, the smaller the overlap between luminance and chrominance in the spectrum of v. So, a crucial parameter, in order to minimize the demosaicking artifacts, is $\|\boldsymbol{\omega}_0\|$, that should be high enough. We remark that if N_1 or N_2 is even, we can optimally place $\boldsymbol{\omega}_0$ on the boundary of the Nyquist band, far away from the zero frequency. So, like in [2], we impose that N_1 be even—the choice of N_2 would yield the same CFAs, up to a rotation of $90^{\mathbf{o}}$. This actually reduces to set $N_1 = 2$, since the frequency of π yields a periodicity of 2 for the pattern of the CFA in the spatial domain. Additionally, this minimal value of N_1 provides us with CFAs having a small repetitive pattern, hence, a small number of different filters, with benefits for the physical realizability of the CFA. Consequently, the modulating frequency takes the form

$$\boldsymbol{\omega}_0 = [\pi, \omega_0]^{\mathrm{T}}, \quad \text{with } \omega_0 = \frac{2\pi n_2}{N_2}, \tag{14}$$

where the integer $n_2 \in (1, \lfloor (N_2 - 1)/2 \rfloor)$ is a free parameter, such that n_2 and N_2 are relatively prime (else, the CFA reverts to a CFA obtained with a lower value of N_2). We can choose $\omega_0 > 0$, since the opposite sign yields the same CFA, up to an horizontal symmetry. We also note that $N_2 \geq 3$, since there is no 2×2 CFA satisfying the six previous criteria.

We can now give the expression of every CFA satisfying the six previous conditions as:

$$\mathrm{cfa}^{L}[\mathbf{k}] = \gamma^L \tag{15}$$

$$\mathrm{cfa}^{C_1}[\mathbf{k}] = \gamma^C (-1)^{k_1} \sqrt{2} \cos(\omega_0 k_2 - \varphi) \tag{16}$$

$$\mathrm{cfa}^{C_2}[\mathbf{k}] = \gamma^C (-1)^{k_1} \sqrt{2} \sin(\omega_0 k_2 - \varphi), \tag{17}$$

where ω_0 is given by (14) and N_2, n_2, γ^L, γ^C, φ are free parameters.

Condition 7) In order to maximize the color discrimination capabilities of the CFA, for given values of N_2, n_2, and γ^L, we impose the chrominance gain γ^C to be maximal, since a high value of γ^C reduces both the demosaicking artifacts (the chrominance information is less polluted by the high frequency content of the luminance) and the level of noise in the chrominance channels of the demosaicked image. After some calculations which are given in the Appendix, we obtain the final form of the CFAs satisfying all the above constraints as:

$$\mathrm{cfa}^{L}[\mathbf{k}] = \gamma^L \tag{18}$$

$$\mathrm{cfa}^{C_1}[\mathbf{k}] = \gamma^C (-1)^{k_1+1} \sqrt{2} \sin(\omega_0 k_2 - \omega_2) \tag{19}$$

$$\mathrm{cfa}^{C_2}[\mathbf{k}] = \gamma^C (-1)^{k_1} \sqrt{2} \cos(\omega_0 k_2 - \omega_2), \tag{20}$$

where

$$\gamma^C = \frac{\sqrt{3} - \gamma^L}{2\cos(\omega_2)}, \tag{21}$$

$$\omega_0 = \frac{2\pi n_2}{N_2}, \qquad \omega_2 = \frac{\pi}{\mathrm{lcm}(6, N_2)}, \tag{22}$$

and lcm denote the least common multiple.

Let us synthesize the ideas of the design process carried out in this section. Using the previous conditions, we derived a new family of CFAs with the following features:

- The CFA has a periodic pattern of arbitrary size $2 \times N_2$ (or $N_2 \times 2$ after rotation).
- The luminance of the scene lies in the low-frequency part of the mosaicked image, with adjustable light sensitivity γ^L.
- The chrominance of the scene lies in the high-frequency part of the mosaicked image. More precisely, the chrominance is the combination of two low-pass signals, modulated in quadrature at the high frequency $\pm\boldsymbol{\omega}_0$, optimally placed on the boundary of the Nyquist band. So, the two chrominance information are fairly encoded the same way, and the CFA does not have a higher color discrimination along some preferential chrominance axis. Consequently, the R, G, and B sensitivities of the CFA are the same.
- The chrominance gain is maximum for a given luminance gain, which means optimal color discrimination capabilities for the CFA. Consequently, the demosaicking artifacts are minimized and the signal-to-noise ratio in the chrominance bands is maximized.

In the next section, we push the optimization constraints further, and tune the remaining degrees of freedom to exhibit a single CFA having the best properties.

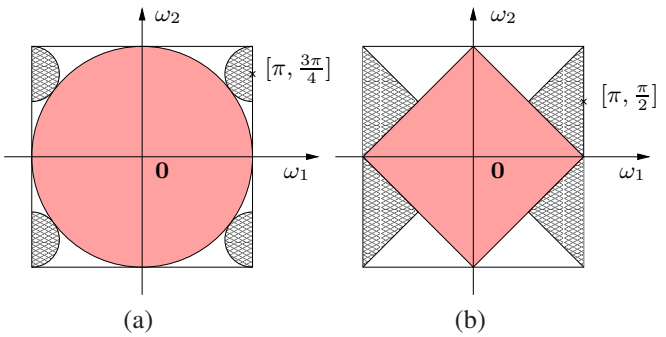

(a) (b)

Fig. 1. If the luminance and two chrominance channels are band-limited, it is possible to modulate the chrominance channels in quadrature at some high frequency so that there is no aliasing. (a) Assuming that the channels are circularly band-limited with maximum bandwidth for the luminance (big circle), the modulating frequency $[\pi, \frac{3\pi}{4}]$ allows the maximum bandwidth for the chrominance (shaded circles). (b) For signals band-limited with diamond shapes, an assumption which more accounts for the predominance of vertically and horizontally aligned content in natural scenes, then the modulating frequency $[\pi, \frac{\pi}{2}]$ allows the maximum bandwidth for the chrominance.

IV. Sensitivity vs. Robustness to Aliasing

Up to this point of the design, we have no indication on how choosing the modulating frequency $\boldsymbol{\omega}_0$. It should be the farthest to the origin—that is, the closest to $[\pi, \pi]^{\mathrm{T}}$—to minimize the aliasing between the luminance and chrominance information. Especially, it should be far from the vertical and horizontal axes, where some energy of the luminance is concentrated, due to the predominance of vertical and horizontal structures in natural scenes. On the other side, if $\boldsymbol{\omega}_0$ is too close to $[\pi, \pi]^{\mathrm{T}}$, aliasing will occur between the two chrominance channels. Indeed, the chrominance content should have a maximal cutoff frequency of $\min(\omega_0, \pi - \omega_0)$ to avoid inter-channel aliasing. In Fig. 1, we show that ω_0 should reasonably be chosen in the interval $[\frac{\pi}{2}, \frac{3\pi}{4}]$, depending on the assumption we make on the power spectra of the luminance and chrominance for typical natural images. Also, Hirakawa showed that the cross-talk effects during acquisition, that are neglected in this work but encountered in practice, desaturate the chrominance information [22]. This amounts to further reduce the chrominance gain of the CFA, and the farther $\boldsymbol{\omega}_0$ from $\mathbf{0}$, the higher this reduction.

Moreover, due to the many problems encountered in practice for manufacturing filters having precisely the required colors, the number of distinct filters should be small. In this respect, the 2×4 pattern (with $N_2 = 4$, $n_2 = 1$, $\omega_0 = \frac{\pi}{2}$) is the best, with only four distinct filters. The size of the pattern should be small too, to simplify the manufacture but also to simplify the design of the demosaicking process and the visibility of some artifacts: when high-frequency content of the chrominance is aliased and misinterpreted as luminance information, zipper artifacts appear with the 2×2 Bayer pattern. With a pattern having a bigger size, the equivalent artifacts may be more visually disturbing, showing a pattern with larger periodicity. The 2×3 pattern is the best one in this respect.

Keeping in mind the previous remarks of this section, we concentrate again on what we consider to be the first and foremost design criterion in this framework; that is, the maximization of the chrominance gain γ^C for a given luminance gain γ^L. We used this criterion in the Condition 7) in the previous section to constrain the admissible solutions, but we can go one step further and also optimize the frequency ω_0 with respect to this requirement. According to Eqns. (21) and (22), we conclude that the optimal pattern is obtained with $N_2 = 3$ (therefore, $n_2 = 1$). Every other pattern in our family has a chrominance gain 10% to 13% lower. This 2×3 pattern is the smallest and it has a small number (six) of distinct filters. Its modulation frequency $\omega_0 = \frac{2\pi}{3}$ is well placed, according to the previous discussion. So, the 2×3 pattern shows up as the best compromise in the whole family.

It should be noted that in practice, the manufacturers put a so-called anti-alias filter on the sensor, a thin layer of a material with blurring properties that acts like a lowpass filter on the continuously-defined color scene $\mathbf{s}(\mathbf{x})$ which is sampled. In other words,

$$\mathbf{im}[\mathbf{k}] = (\mathbf{s} * g)(T\mathbf{k}) \quad \forall \mathbf{k} \in \mathbb{Z}^2, \tag{23}$$

where T is the sampling step and g is the lowpass filter modeling the combined effect of the anti-alias filter, the micro-lenses and the integration over the photo-sensitive surface of each sensor pixel (assuming that the optical system is good enough and is not the limiting factor of the resolution). The anti-alias filter is chosen so that the cut-off frequency of g appropriately limits the bandwidth of the luminance and chrominance before sampling. Thus, there is no aliasing between them after sampling. That is why we almost never see, in pictures acquired with digital cameras, the typical color fringes which are described in the academic literature of demosaicking. The price to pay for removing the visually disturbing artifacts due to aliasing is a loss of resolution[1]. This means that the demosaicked image is over-sampled: its frequency-content does not occupy the whole available bandwidth, since the high-frequencies of the color scene have been removed more than required to match the Nyquist frequency associated to the sensor geometry. So, the whole discussion about the amount of distortion due to aliasing should be turned into a discussion about the actual resolution of the demosaicked image. We leave the detailed analysis of the intricate relationships between robustness to aliasing, sensitivity properties, sensor resolution, noise level, cross-talk effects, and the resulting image quality, to future publications, since this goes far beyond the scope of this paper. We refer to [6] on this topic. To conclude this point, we just have to keep in mind that a CFA less prone to luminance/chrominance aliasing than the Bayer CFA allows to capture the same visual information, using a sensor of given size having a lower pixel count.

V. Demosaicking Strategy

A. A Generic Linear Approach to Demosaicking for the New CFAs

Our CFAs have a natural and simple demosaicking algorithm associated to them, inspired by their characteristics in

[1]but this is a relevant choice: to quote a remark in [2], "although it is a well-accepted fact that our visual systems are less sensitive to changes in color than changes in brightness, manifestation of colors utterly irrelevant to the scene stand out more than minor alterations in brightness".

the Fourier domain. This demosaicking process amounts to separate the frequency content of the mosaicked image into the luminance and chrominance channels of the reconstructed image. For this, we first estimate the chrominance and then subtract it to the mosaicked image v to obtain the luminance. The chrominance is obtained by re-modulating v so that the chrominance is shifted in the low frequency area, and then applying a low-pass convolution. So, the complexity of the demosaicking process is basically limited to two convolutions! In addition, they use the same filter and can be performed in parallel.

More precisely, the demosaicking method proposed consists in the following steps, where we denote by $\widetilde{\mathbf{im}}$ the demosaicked image, that aims at estimating $\mathbf{im}$.

1) Compute the image v_1 from v by modulation with the carrier wave of the chrominance C_1: $v_1[\mathbf{k}] = (-1)^{k_1+1}\sqrt{2}\sin(\omega_0 k_2 - \omega_2)/\gamma^C\, v[\mathbf{k}]$.
2) Apply the convolution with the appropriate low-pass filter h: $\widetilde{\mathrm{im}}^{C_1} = v_1 * h$.
3) Compute the image v_2 from v by modulation with the carrier wave of the chrominance C_2: $v_2[\mathbf{k}] = (-1)^{k_1}\sqrt{2}\cos(\omega_0 k_2 - \omega_2)/\gamma^C\, v[\mathbf{k}]$.
4) Apply the convolution with the same low-pass filter h: $\widetilde{\mathrm{im}}^{C_2} = v_2 * h$.
5) Estimate the luminance by subtraction of the remodulated chrominance: $\widetilde{\mathrm{im}}^{L}[\mathbf{k}] = \Big(v[\mathbf{k}] - \gamma^C(-1)^{k_1+1}\sqrt{2}\sin(\omega_0 k_2 - \omega_2)\,\widetilde{\mathrm{im}}^{C_1}[\mathbf{k}] - \gamma^C(-1)^{k_1}\sqrt{2}\cos(\omega_0 k_2 - \omega_2)\,\widetilde{\mathrm{im}}^{C_2}[\mathbf{k}]\Big)/\gamma^L$.
6) Compute $\widetilde{\mathrm{im}}^{R}, \widetilde{\mathrm{im}}^{G}, \widetilde{\mathrm{im}}^{B}$ by change of basis from $\widetilde{\mathrm{im}}^{C_1}, \widetilde{\mathrm{im}}^{C_2}, \widetilde{\mathrm{im}}^{L}$.

In practice, the values of the carrier waves should be precomputed in a look-up table of size $2N_2$, to exploit their periodicity. We also remark that it is equivalent to directly estimate the luminance from v by convolution: we have $\widetilde{\mathrm{im}}^{L} = v * g$, where $g[\mathbf{k}] = \big(\delta_{\mathbf{k},\mathbf{0}} - 2(-1)^{k_1}\cos(\omega_0 k_2)h[\mathbf{k}]\big)/\gamma^L$ and the Kronecker symbol is defined by $\delta_{x,y} = \{1 \text{ if } x = y, 0 \text{ else}\}$. This possibility may be interesting if the luminance is to be computed in parallel with the chrominance.

If cross-talk has to be taken into account and corrected, the method proposed in [22] simply amounts to multiplying $\widetilde{\mathrm{im}}^{C_1}$ and $\widetilde{\mathrm{im}}^{C_2}$ by some constant between steps 5 and 6.

The proposed algorithm can be easily adapted to handle other CFAs. It turns out that our algorithm does the same, but more efficiently, as the generic approach of Hirakawa *et al.* [2], [4]. In particular, for their 2×4 CFA, our algorithm can be used, by putting the appropriate values for the gains and the modulating frequencies (see Sect. VI-A). The algorithm can also be adapted for the Bayer CFA; this exactly yields the linear algorithm of Dubois [9]. Note that with CFAs other than the new ones proposed in this work, the estimation of the luminance is not equivalent to a convolution any more. This makes the analysis of the process in noisy situations and the development of efficient denoising strategies more difficult.

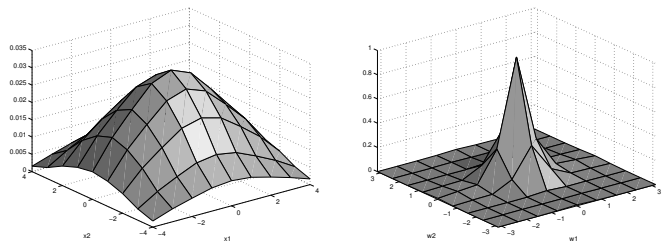

(a) (b)

Fig. 2. The 9×9 filter used for estimating the chrominance, optimal in the least-squares sense, for the proposed 2×3 CFA (depicted as CFA (VI) in Fig 3) (a) and its spectrum (b).

The choice of the filter h still has to be discussed. It is possible to use, like in [4], a short separable filter, with zeros at ω_0 and $2\omega_0$ for the vertical filter and at π for the horizontal one. In this work, for comparison purpose between the CFAs, we use in Sect. VI for every CFA the non-separable 9×9 filter(s) optimal in the least-squares sense. That is, we minimize the error $\|\mathbf{Ax} - \mathbf{b}\|^2$, where $\mathbf{x}$ is the vector containing the 81 coefficients, in lexicographic order, of the filter h we are seeking; $\mathbf{A}$ is the matrix whose each row contains the 81 chrominance values for every 9×9 patch of the mosaicked images in the whole test set of 20 images; $\mathbf{b}$ is the vector containing the true chrominance values for the corresponding center pixel of the patch. It is known that the solution of this standard linear algebra problem has the form $\mathbf{x} = (\mathbf{A}^{\mathrm{T}}\mathbf{A})^{-1}\mathbf{A}^{\mathrm{T}}\mathbf{b}$. So, the LS-optimal filters are solutions of 81×81 linear systems, which have to be solved off-line only once for every CFA. The filter h obtained for our CFA (VI) is depicted in Fig. 2. For the Bayer filter, we computed for the C_3 chrominance (see Sect. VI-A) the filter such that, when applied at $[\pi, 0]^{\mathrm{T}}$ and its transpose at $[0, \pi]^{\mathrm{T}}$, the estimation based on the average of the two results is optimal in the LS sense.

Therefore, by using the LS-optimal filters, we are able to exploit at best the intrinsic properties of the CFAs. The combination of the generic linear framework based on spectral selection and the optimal filters associated to each CFA provides a fair and robust way for comparing the performances of CFAs.

B. Behavior in Noisy Conditions

The linearity of the demosaicking process is a very important property in the case the mosaicked image is corrupted by sensor noise. The linearity allows to precisely describe the behavior of the noise throughout the process and to develop efficient strategies for subsequent denoising or for joint demosaicking/denoising. On the contrary, non-linear demosaicking approaches may provide better results in ideal noiseless conditions, but their mechanisms use properties of the image that may be not exploitable any more in the noisy case. In addition to this lack of robustness, they distort the noise characteristics, so that denoising is made much harder. Since the study of joint demosaicking and denoising would go far beyond the scope of this paper, we limit our analysis to

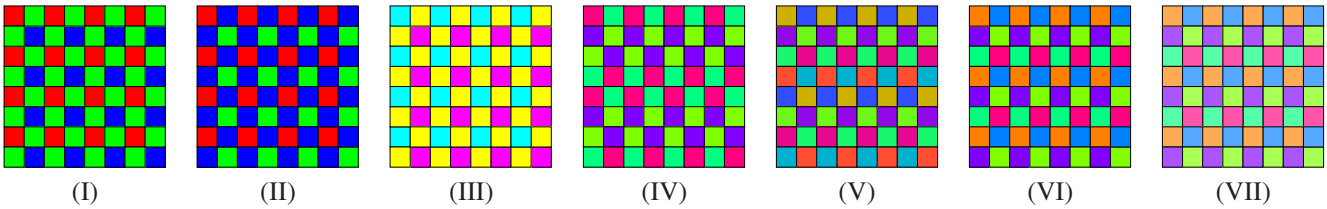

Fig. 3. The seven CFAs used in our experiments. (I): Bayer pattern [10], (II): Bayer pattern with permuted G and B channels, (III): CMY pattern [10], (IV): Hirakawa pattern [1], [2] ($\gamma^L = \frac{\sqrt{3}}{2}$), (V): proposed 2×8 pattern ($\gamma^L = \frac{\sqrt{3}}{2}$), (VI): proposed 2×3 pattern ($\gamma^L = \frac{\sqrt{3}}{2}$), (VII): proposed 2×3 pattern with higher luminance gain ($\gamma^L = \frac{2}{\sqrt{3}}$, like for the CMY pattern).

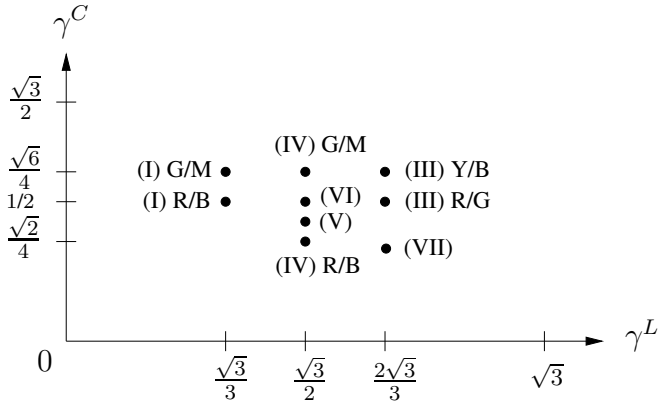

Fig. 4. Luminance and chrominance gains for the CFA depicted in Fig. 3.

the behavior of noise throughout the proposed demosaicking process, denoted by $\mathcal{D}$ thereafter

Since $\mathcal{D}$ is linear, applying it to the mosaicked image $v_n = v + \varepsilon$ corrupted by additive noise yields the noisy demosaicked image $\widetilde{\mathbf{im}}_n = \mathcal{D}v + \mathcal{D}\varepsilon = \widetilde{\mathbf{im}} + \mathcal{D}\varepsilon$. Therefore, the problems of demosaicking and denoising are separable: we can leave the demosaicking process unchanged in presence of noise and concentrate on the denoising task which consists in estimating $\widetilde{\mathbf{im}}$ from $\widetilde{\mathbf{im}}_n$, performed after demosaicking. Let us focus on the characteristics of the color noise $\boldsymbol{\varepsilon} = \mathcal{D}\varepsilon$, in the case ε is a realization of a white Gaussian stationary random process with zero mean and standard deviation σ. Then, we obtain the following results after some calculations, under the assumption that the lowpass filter h is bandlimited with cutoff frequency $\min(\omega_0, \pi - \omega_0)$:

- The three bands ε^L, ε^{C_1}, ε^{C_2} of $\boldsymbol{\varepsilon}$ are statistically independant.
- ε^{C_1} and ε^{C_2} are realizations of a Gaussian stationary random process with zero mean and power spectrum density $\frac{\sigma^2}{(\gamma^C)^2}|\hat{h}(\boldsymbol{\omega})|^2$.
- ε^L is a realization of a Gaussian stationary random process with zero mean and power spectrum density $\sigma^2|\hat{g}(\boldsymbol{\omega})|^2 = \frac{\sigma^2}{(\gamma^L)^2}|1 - \hat{h}(\boldsymbol{\omega} - \boldsymbol{\omega}_0) - \hat{h}(\boldsymbol{\omega} + \boldsymbol{\omega}_0)|^2$.

Thus, since the channels of $\widetilde{\mathbf{im}}$ are also independent in the L, C_1, C_2 basis, the denoising problem is separable: we can denoise the three channels of $\mathbf{im}_n$ in this basis, independently. This task is made difficult by the fact that the noise is not white, however.

VI. Performance analysis

A. The CFAs Under Comparison

In order to evaluate the performances of our new designs, we consider the seven CFAs depicted in Fig. 3. To compare their characteristics, we first define another orthonormal luminance/chrominance basis:

$$L = \frac{1}{\sqrt{3}}[1,1,1]^{\mathrm{T}}, C_3 = \frac{1}{\sqrt{2}}[-1,0,1]^{\mathrm{T}}, C_4 = \frac{1}{\sqrt{6}}[-1,2,-1]. \tag{24}$$

Then, the seven CFAs under comparison are:

- (I). The well-known Bayer CFA [10]. It has $\gamma^L = 1/\sqrt{3}$. The chrominance C_4 is modulated at $\boldsymbol{\omega}_0 = [\pi, \pi]^{\mathrm{T}}$ with $\gamma^{C_4} = \sqrt{6}/4$ and the chrominance C_3 is modulated at $[0, \pi]^{\mathrm{T}}$ and $[\pi, 0]^{\mathrm{T}}$. The chrominance gain γ^{C_3} can be defined by extension, from the amplification value of the noise level after demosaicking by spectral selection and averaging of these two replicas. This yields $\gamma^{C_3} = 1/2$.
- (II). The Bayer CFA, whose green and blue filters have been exchanged, to validate the intuition given in [8] that this variant should perform better than the Bayer CFA. In fact, the spectral overlap between luminance and the chrominance C_3 is decreased, since there is in average less energy in the $R-G$ than in the $R-B$ chrominance band in natural images. The gains are the same as for the Bayer CFA, considering a decomposition in C_1 and C_2 instead of C_3 and C_4.
- (III). The CMY pattern, a variant of the Bayer CFA with doubled light sensitivity ($\gamma^L = 2/\sqrt{3}$) [10]. To our knowledge, no advanced demosaicking method was proposed for it in the literature. This CFA is the reversed version of the CFA (II) (see Condition 5) in Section III); so, their chrominance gains are the same. Therefore, the linear and non-linear demosaicking methods based on spectral selection, like in [8], [9], can be applied to this CFA the same way, after only changing some constant values in the algorithms.
- (IV). The pattern of type 1 recently designed by Hirakawa *et al.* [1], [2]. It consists in filters with the colors $[\frac{1}{2}, 1, 0]$, $[0, 1, \frac{1}{2}]$, $[1, 0, \frac{1}{2}]$ and $[\frac{1}{2}, 0, 1]$ arranged with a 2×4 periodicity. The results reported in [1], [2] makes this CFA the best proposed to date. Its luminance gain is $\gamma^L = \sqrt{3}/2$. The chrominance C_3 is modulated at $\boldsymbol{\omega}_0 = [\pi, \pi]^{\mathrm{T}}$ with $\gamma^{C_3} = \sqrt{2}/4$ and the chrominance C_4 is modulated at $\boldsymbol{\omega}_0 = [\pi, \pi/2]^{\mathrm{T}}$ with $\gamma^{C_4} = \sqrt{6}/4$. This CFA has been obtained by maximizing the total chrominance energy $\left(\gamma^{C_3}\right)^2 + \left(\gamma^{C_4}\right)^2$ among all possible patterns of size 2×4.

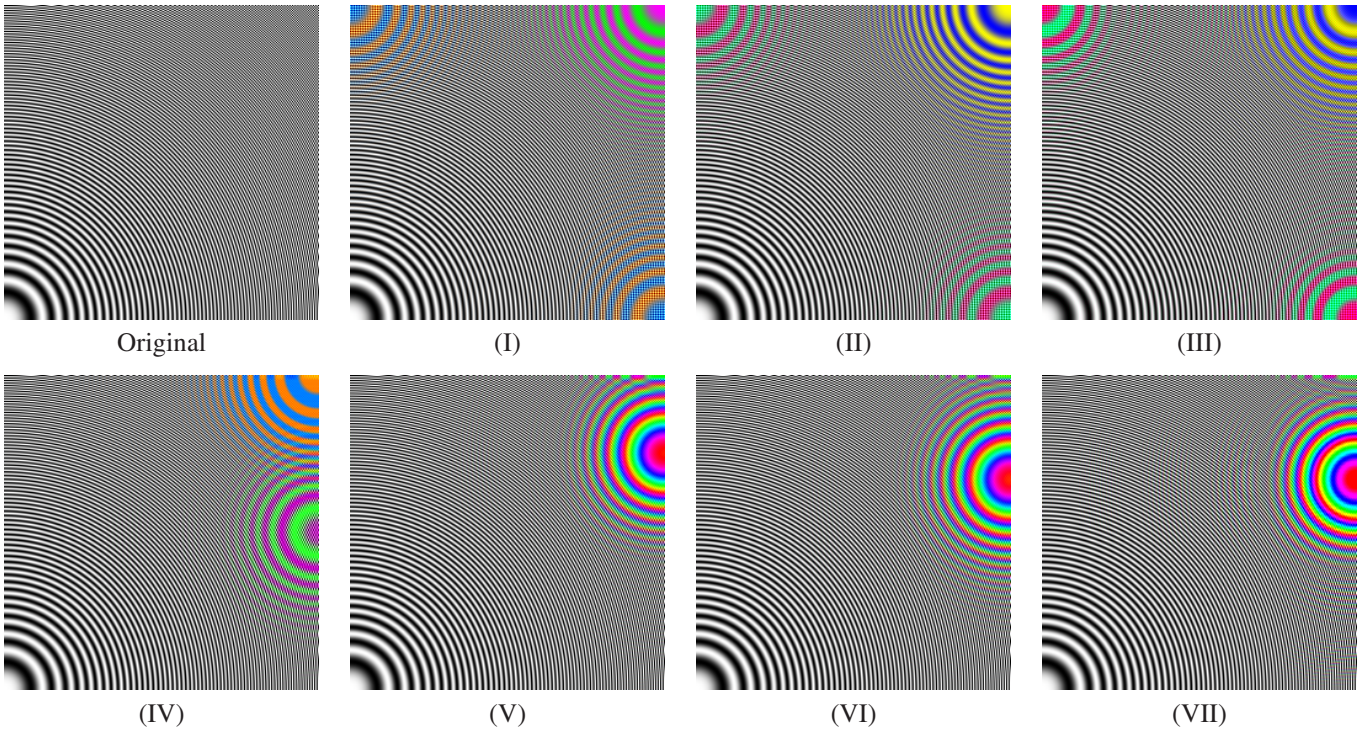

Fig. 5. Results of our demosaicking method used with the seven CFAs depicted in Fig. 3, on a grayscale synthetic zoneplate pattern.

- (V). The proposed 2×8 pattern with $\gamma^L = \sqrt{3}/2$, which has chrominance modulated at $\boldsymbol{\omega}_0 = [\pi, 3\pi/4]^{\mathrm{T}}$ with $\gamma^C \approx 0.433$.
- (VI). The proposed 2×3 pattern with $\gamma^L = \sqrt{3}/2$, which has chrominance modulated at $\boldsymbol{\omega}_0 = [\pi, 2\pi/3]^{\mathrm{T}}$ with $\gamma^C = 1/2$. This CFA is made of filters with the colors $[1, 0, \frac{1}{2}]$, $[1, \frac{1}{2}, 0]$, $[0, 1, \frac{1}{2}]$, $[0, \frac{1}{2}, 1]$, $[\frac{1}{2}, 0, 1]$ and $[\frac{1}{2}, 1, 0]$.
- (VII). The proposed 2×3 pattern with higher luminance gain $\gamma^L = 2/\sqrt{3}$, like the CFA (III). Its chrominance gain is $\gamma^C = 1/3$.

The luminance and chrominance gains of these CFAs are summarized in Fig. 4. We first remark that the CFAs (I)–(III) have maximal chrominance gains for their respective luminance gains, since they are made of filters having maximally saturated colors. Secondly, the CFAs (IV) and (VI) have the same chrominance energy captured in the mosaicked image: $\left(\gamma^{C_3}\right)^2 + \left(\gamma^{C_4}\right)^2 = 1/2$ in both cases. However, this is obtained for the CFA (IV) at the cost of a strong asymmetry between the two color components: $\gamma^{C_4}/\gamma^{C_3} = \sqrt{3}$. This means that noise is much more amplified in the $B - R$ band than in the $G - M$ band after demosaicking. Also note that for the CFAs (III) to (VI), increasing γ^L simply amounts to take a linear combination of the CFA with the transparent CFA ($\mathbf{cfa}[\mathbf{k}] = [1, 1, 1]^{\mathrm{T}}\ \forall \mathbf{k}$). So, the chrominance gains are reduced in the same extent. Since these gains are already smaller than γ^L, which indicates a higher amplification of chrominance noise than luminance noise during demosaicking, γ^L should be maintained at its smallest value. So, the CFA (VII) is given only for illustration purpose; in comparison with the CFA (VI), it is more sensitive to luminance/chrominance aliasing and the chrominance noise is even more amplified.

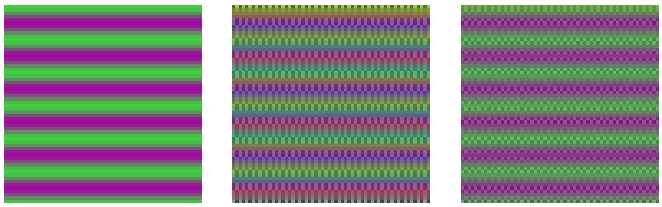

Fig. 6. Demosaicking results for the synthetic image (a), which consists in a sine with pulsation $\pi/5$ oscillating between green and magenta. With the CFA (IV) of Hirakawa *et al.* (b), aliasing between the two chrominance bands appears, while with our CFA (VI) (c), there is only aliasing between the chrominance and the luminance.

To visually illustrate the modulation of the chrominance in the Fourier domain by the CFAs, we give in Fig. 5 the images obtained when a synthetic zoneplate is mosaicked and demosaicked with the proposed method. These images show how the demosaicking method assigns the frequency content of the mosaicked image—equal in this case to the initial zoneplate, since it is gray-valued—to the luminance or chrominance bands of the reconstructed color image. Thus, we can see at which frequencies aliasing occurs and to which extent. For instance, we see that the CFA (IV) is sensitive to aliasing between the two chrominance bands. This may be visible in demosaicked natural images at sharp color transitions for horizontally aligned objects. This effect is illustrated by a synthetic example in Fig. 6.

B. Evaluation in Noiseless Situations

For experimental validation purpose, we consider the data set of 20 color images of size 768×512 used by many authors to test their methods (e.g. [2], [23]). These images

TABLE I

MSE FOR THE LINEAR DEMOSAICKING EXPERIMENTS USING DIFFERENT CFAS, IN THE NOISELESS CASE. IMAGE NUMBERS CORRESPOND TO [23].

Demosa. method	Non-linear [9]	Non-linear [24]	Proposed linear demosaicking framework with 9×9 LS-optimal filters						
CFA	Bayer	Bayer	Bayer	Bayer $G \Leftrightarrow B$	CMY	Hirakawa [1], [2]	2×8 $\gamma^L = \frac{\sqrt{3}}{2}$	2×3 $\gamma^L = \frac{\sqrt{3}}{2}$	2×3 $\gamma^L = \frac{2}{\sqrt{3}}$
1	10.12	11.45	12.93	12.85	21.24	**6.53**	6.60	7.12	12.03
2	6.80	5.75	7.92	8.17	12.53	**6.01**	7.42	7.07	10.02
3	10.56	10.14	13.14	**11.59**	14.79	12.58	13.07	13.38	20.22
4	6.47	10.15	10.26	8.84	13.65	**4.80**	5.09	5.32	8.73
5	4.00	5.02	3.34	**4.40**	5.91	4.59	5.03	4.53	6.64
6	19.31	19.26	29.25	26.28	46.55	**10.92**	11.42	11.90	18.38
7	3.96	3.38	5.16	4.39	6.03	**3.88**	4.15	4.00	5.79
8	3.91	3.56	4.42	4.01	4.73	**3.57**	3.70	3.58	5.03
9	6.80	7.49	8.74	8.30	11.77	**5.76**	6.18	6.14	9.54
10	3.20	3.39	4.17	4.05	6.36	2.93	2.95	**2.92**	4.09
11	19.98	27.03	20.39	18.74	25.10	16.87	**16.05**	17.90	31.44
12	7.35	7.08	7.82	8.40	10.36	**7.06**	7.40	7.36	9.80
13	2.77	4.92	5.26	4.47	7.08	**2.10**	2.17	2.15	3.33
14	4.42	4.66	4.69	4.21	4.85	**4.14**	4.30	4.54	6.79
15	12.05	13.01	12.42	11.50	13.50	**11.15**	11.59	11.81	18.37
16	5.92	6.30	10.06	8.77	14.69	**4.48**	4.73	4.87	7.47
17	5.92	5.04	6.11	4.77	5.60	**4.64**	4.93	5.05	7.29
18	8.51	8.72	9.34	8.13	12.15	**5.59**	5.90	6.04	9.62
19	9.86	9.00	10.78	9.84	12.97	**8.48**	8.94	8.81	11.84
20	18.94	21.42	19.29	16.70	18.67	**14.24**	14.92	15.44	20.39
Mean	8.54	9.25	10.36	9.42	13.43	7.02	7.33	7.50	11.34

were mosaicked using the considered CFAs and demosaicked using spectral selection, as discussed in Sect. V. We caution the reader that image quality after reconstruction depends on the demosaicking method used, but the aim of this article is not the optimization of demosaicking *per se*. The generic and robust paradigm of spectral selection provides reliable qualitative insights into the difference of image quality that can be expected when using one or the other CFA. Note that to simulate an acquisition with a real camera, all images were put in landscape mode; that is, the vertical images were turned 90° left. Indeed, vertical pictures are taken by rotating the camera, so that the scene presented to the sensor is rotated in that case.

The mean squared errors (MSE)[2] obtained are reported in Tab. I. In the first two columns, we also report the results obtained for the Bayer CFA with two state-of-the-art non-linear demosaicking methods[3], to illustrate the gains that can be expected when non-linearly exploiting the redundancy of the $B - R$ chrominance modulated at $[0, \pi]^{\mathrm{T}}$ and $[\pi, 0]^{\mathrm{T}}$ for this CFA. Such improvements can not be expected for the CFAs (IV) to (VII) since each chrominance channel is modulated at only one frequency. Also, these improvements can be achieved because of the noiseless assumption. In the more realistic case where the mosaicked image is corrupted by noise, it is doubtful that the redundancy can be exploited any more, since the mechanisms involved, based on local orientation detection, are sensitive to noise. Moreover, the non-linear demosaicking methods distort the characteristics of noise, which makes subsequent denoising a much more difficult task. As result, the MSE improvement of at most 18% obtained with the non-linear methods over our linear approach is not so significant, especially when taking into account the much higher computation cost.

Since the MSE results may not be sufficient to evaluate the quality of the demosaicked images, we also provide illustrations in Fig. 7. We have to keep in mind that the objective of commercial photography is not so much the accurate reproduction of a scene, but delivering visually pleasant images without noticeable artifacts. From the numerical and visual results, the following observations can be made:

- The best results are obtained with the CFA (IV). The CFA (V) and (VI) are slightly worse, but these three CFAs largely outperform the Bayer CFA, even when non-linear demosaicking is used. The typical color fringes (see the fence) and zipper effects (see the red bow) that occur with the CFAs (I)–(III) disappear with the CFAs (IV)–(VII). This is due to the property that with the new CFAs, the chrominance is modulated farther away from the origin and not on the horizontal and vertical axes of the frequency plane, where much energy is present because of the predominance in natural images of structures aligned along these two canonical directions.
- In real acquisition conditions, with the CFAs (IV)–(VI), there would not be artifacts like the ones slightly visible in Fig. 7, since the resolution of the whole acquisition system for oblique angles rarely matches the resolution

[2]The MSE between $\mathbf{im}$ and $\widetilde{\mathbf{im}}$ for images of size $N \times M$ is

$$\mathrm{MSE} = \frac{1}{3NM} \sum_{\mathbf{k} \in [1..N] \times [1..M]} \sum_{X \in \Omega} \left| \mathbf{im}^X[\mathbf{k}] - \widetilde{\mathbf{im}}^X[\mathbf{k}] \right|^2, \qquad (25)$$

for $\Omega = \{R, G, B\}$ or $\Omega = \{L, C_1, C_2\}$. However, in this article, like in [2], we do not take into account the first and last five rows and columns of the demosaicked images for the computation of the MSE, since the initial images used for the tests have been badly acquired at the boundaries.

[3]For the method of Dubois [9], we computed the MSE using the images available online at
`http://www.site.uottawa.ca/~edubois/demosaicking/`.

For the method of Nai-Xiang *et al.* [24], we performed the demosaicking experiments using the Matlab code put available online by the authors at
`http://www.ntu.edu.sg/home5/CHAN0069/AFdemosaick.zip`

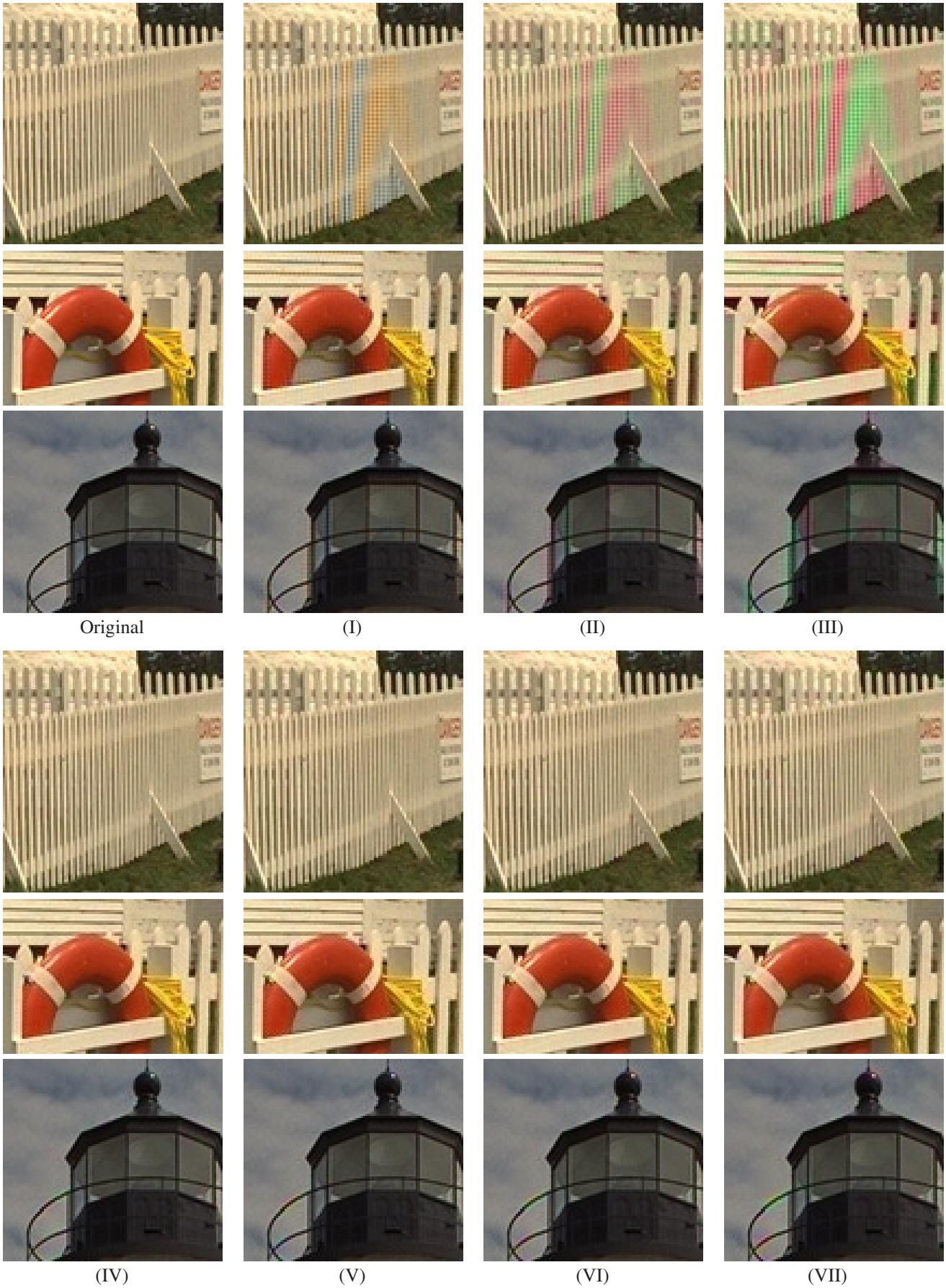

Fig. 7. Results of our demosaicking method used with the seven CFAs depicted in Fig. 3, on three parts of the *Lighthouse* image (image number 16 in Tab. I). The image was rotated before mosaicking and rotated back after demosaicking, to simulate acquisition with a sensor aligned for landscape images.

of the sensor (in other words, we are in a situation like in Fig. 1). Therefore, the anti-alias filter in front of the sensor required with the Bayer CFA is not necessary any more with the new CFAs.

- The CFAs (III) and (VII) with larger luminance gain yield the worst performances. This confirms the property that the ratio γ^C/γ^L must not be too small; else, the chrominance is polluted by the high frequencies of the luminance. Indeed, the fringes visible with the Bayer CFA have an even higher intensity with the CFA (III), at every location in the image where a sharp transition is present. For the CFA (VII), the aliasing artifacts take the form of rainbow halos around sharp transitions oriented at $\pm \arctan(3/2) \approx \pm 56^\circ$ with respect to the horizontal axis. These artifacts are the same for the CFAs (V) and (VI), but with lower intensity.
- With the CFA (IV), the artifacts are present around transitions with more orientations than with the CFAs (V) and (VI), but with lower intensity, and they take the form of bicolored instead of rainbow-like halos. In fact, only one half of the frequency content of the mosaicked image around $\pm[\pi, \pi/2]^{\mathrm{T}}$ has to be shared between luminance and G/M chrominance during demosaicking. The remaining energy, at the same frequency but with phase in quadrature, corresponds to luminance information. This property, visible in Fig. 5, explains why the CFA (IV) slightly outperforms the CFAs (V) and (VI), whose modulating frequency $\boldsymbol{\omega}_0$ is farther from zero, but with two times more energy around $\boldsymbol{\omega}_0$, potentially aliased.
- The observation in [8] that exchanging the blue and green filters of the Bayer CFA improves the performances is confirmed, with an average 9% decrease of the MSE.

C. Evaluation in Noisy Situations

The ideal noiseless scenario does not realistically represent real acquisition conditions. The sensor always delivers data corrupted by noise, and the noise level is amplified by the analog gain (corresponding to the choice of the ISO sensitivity in the camera) applied to the sensor output before A/D conversion [16]. In Fig. 8, we give examples of images demosaicked with our approach, when the mosaicked image is corrupted by additive white Gaussian noise of standard deviation $\sigma = 20$. We first observe that for every CFA, most of the demosaicked noise is concentrated in the luminance. In fact, following the analysis in Sect. V-B, we can write, for our new CFAs, the mean square error MSE_n between the reference image and the noisy demosaicked image $\widetilde{\mathbf{im}}_n$ as

$$\mathrm{MSE}_n = \mathrm{MSE} + \frac{\sigma^2}{3}\left(\frac{1}{(\gamma^L)^2}\left(2\|h - \delta_{\mathbf{0}}\|^2 - 1\right) + \frac{2}{(\gamma^C)^2}\|h\|^2\right). \quad (26)$$

where $\delta_{\mathbf{0}}$ stands for the identity filter. For instance, with the CFA (VI) and the adopted 9×9 lowpass filter h, this yields $\mathrm{MSE}_n = \mathrm{MSE} + 0.45\sigma^2$, with 86% of the noise energy in the luminance of $\widetilde{\mathbf{im}}_n$. Such an analytical study of the noise characteristics can be carried out for the other CFAs, but the analysis is more complicated, since the two chrominance bands are not modulated at the same frequency. Therefore, we provide in Fig. 9 the results of numerical simulations showing the MSE increase as a function of the noise level σ. Of course, a denoising method would be applied in real applications, but the hierarchy between the CFAs should remain the same, before and after denoising.

We can do the following observations:

- The CFAs (I)–(III) have the same lowest level of chrominance noise, since they have the highest chrominance gains.
- The CFAs (III) and (VII) have the same lowest level of luminance noise, but the chrominance noise is reduced with the CFA (III).
- We can see the influence of increasing γ^L by comparing the results of the CFAs (VI) and (VII). The second one has less luminance noise, but more chrominance noise, which may be difficult to remove since it is lowpass.
- The CFAs (IV), (V), (VI) have the same level of luminance noise, and they outperform the Bayer CFA for every σ.
- The differences between the CFAs (IV), (V), (VI) may be difficult to see visually in the example of Fig. 9, but there is more noise in the B/R than in the G/M chrominance channel of $\widetilde{\mathbf{im}}_n$ for the CFA (IV). This asymmetry is not present with our new CFAs.
- As soon as $\sigma > 5$, the CFAs (V) and (VI) outperform the CFA (IV); indeed, the MSE with the CFA (VI) is 5% lower than with the CFA (IV), which is penalized by the asymmetry of its two chrominance gains.

These properties have to be confronted with the expectations from the imaging system of a digital camera. Depending on the luminosity conditions, different amplification gains (corresponding to the choice of the ISO sensitivity) are used. The image quality is expected to be the best possible at the native sensitivity (e.g. ISO 100) and, secondly, the best possible at high ISO sensitivities. Hence, the best CFA depends on the noise level of the sensor: at the base sensitivity, the sensors available in reflex cameras deliver almost noise free images, while the sensor of a cheap camera phone is noisy even at the minimum usable ISO sensitivity. To summarize, for a cheap noisy sensor (with $\sigma > 6$ for every ISO choice), the CFA (III), which has been neglected so far in the literature, is, unexpectedly, the best choice, since its (γ^L, γ^C) tradeoff is the best in noisy conditions. On the other hand, the CFA (VI) shows up as the best compromise for reflex cameras, since its performances are globally the best in the whole range of noise levels.

VII. Conclusion

In this work, we redefined the problem of CFA design as the maximization of the energy of the color scene captured in the mosaicked image, through the choice of the luminance and chrominance gains of the CFA. We derived the analytical solution to the optimization of these key parameters, under the spectral separation constraint that the chrominance be modulated far away from the luminance in the Fourier domain, as advocated recently by Hirakawa *et al.* [2]. Thus, we provide

Fig. 8. Results of our demosaicking method used with the seven CFAs depicted in Fig. 3, on a part of the *Lighthouse* image. The mosaicked image is corrupted by additive white Gaussian noise of standard deviation $\sigma = 20$ and no denoising process is applied.

a constructive method for designing CFAs within the generic framework of these authors. Consequently, we proposed a whole class of new CFAs with optimal spectral properties. The pattern with the smallest 2×3 periodicity (CFA (VI) in Fig. 3) turns out to be the best compromise; it offers improved robustness to aliasing artifacts and to noise in comparison with the Bayer CFA. A sensor (with given size, geometry, pixel count) equipped with this new CFA would provide images with higher perceived resolution (better definition of small details, since the anti-alias filter can be removed) and better overall quality (the lower level of noise allows the use of a less destructive denoising method). Moreover, the linear demosaicking method proposed, which fully exploits the properties of the CFA, allows to significantly reduce the hardware complexity. In comparison with the designs of Hirakawa *et al.* [2], the two chrominance bands are modulated even farther from the origin and at the same frequency, which slightly improves the robustness to noise and inter-chrominance aliasing.

This article focused on the design of CFAs with optimal theoretical performances, but this is only the first stone in the development of a whole imaging pipeline. We are confident that the spectral properties of the proposed CFAs would benefit to every of its steps, like white-balancing and tone mapping [25], but this is still to be demonstrated. In particular, the design of efficient joint demosaicking/denoising strategies is an open issue, which we are currently investigating.

The proposed framework may also be used for multispectral imaging, e.g. for remote sensing systems which acquire more than three bands in the visible and infrared wavelengths.

APPENDIX I
MAXIMIZATION OF THE CHROMINANCE GAIN

To optimize the chrominance gain γ^C, we proceed in two steps: 1) given φ, we maximize γ^C and 2) we choose φ so that the previously determined γ^C is maximal. For this, let us write cfa^i, $i = 0, 1, 2$ instead of cfa^X, $X = L, C_1, C_2$, respectively. By expanding the equality $\mathbf{cfa} = \mathrm{cfa}^L L + \mathrm{cfa}^{C_1} C_1 + \mathrm{cfa}^{C_2} C_2$,

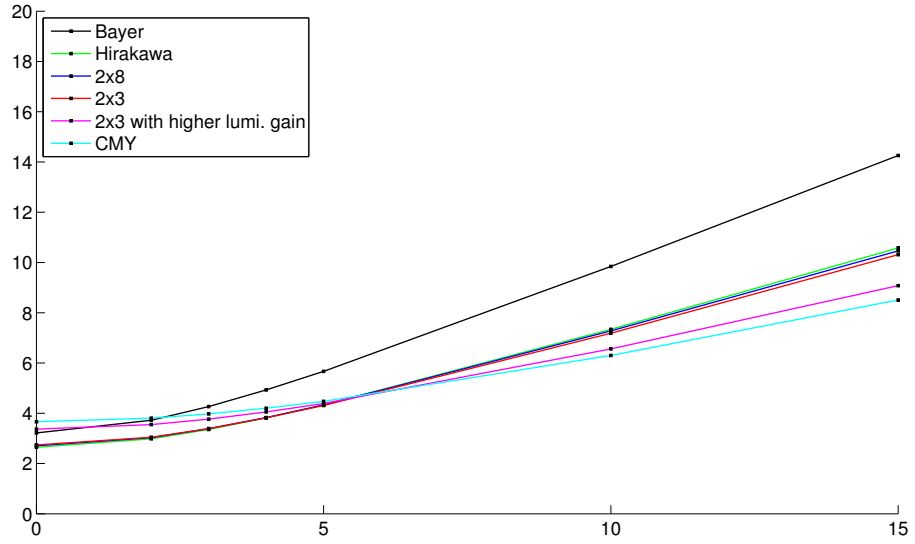

Fig. 9. Square root of the average MSE over the 20 images in function of the standard deviation of the noise σ, after demosaicking in noisy situation with the different CFAs in test. The sequence of the names in the caption, from top to bottom, corresponds to the hierarchy of the curves, for high values of σ.

we obtain:

$$\begin{aligned}\mathrm{cfa}^i[\mathbf{k}] = \frac{\gamma^L}{\sqrt{3}} + \gamma^C(-1)^{k_1}\sqrt{2}\left(\frac{2}{\sqrt{6}}\sin\Big(\frac{2\pi}{3}(2-i)\Big)\right.\\ \times\cos(\omega_0 k_2-\varphi)\\ \left.+\frac{2}{\sqrt{6}}\cos\Big(\frac{2\pi}{3}(2-i)\Big)\sin(\omega_0 k_2-\varphi)\right) \quad (27)\\ = \frac{\gamma^L}{\sqrt{3}} + \frac{2}{\sqrt{3}}\gamma^C(-1)^{k_1}\sin\Big(\frac{2\pi}{3}(2-i)+\omega_0 k_2-\varphi\Big). \quad (28)\end{aligned}$$

Let us define the set

$$\begin{aligned}\Omega = \left\{\left|\sin\Big(\frac{2\pi}{3}(2-i)+\omega_0 k_2-\varphi\Big)\right| \;;\; i,k_2\in\mathbb{Z}\right\} \quad (29)\\ =\big\{|\sin(\omega_1 k-\varphi)| \;;\; k\in\mathbb{Z}\big\}, \quad (30)\end{aligned}$$

where

$$\omega_1 = \gcd\Big(\omega_0,\frac{2\pi}{3}\Big) = \frac{2\pi}{\mathrm{lcm}(3,N_2)}, \quad (31)$$

and $\gcd$ and lcm denote the greatest common divisor and the least common multiple, respectively.

Since $\gamma^L > \sqrt{3}/2$ after Condition 5), the limiting factor for maximizing γ^C is the set of constraints $\mathrm{cfa}^i[\mathbf{k}] \le 1$ for every $i,\mathbf{k}$. Then, maximizing γ^C under these constraints amounts to choose γ^C such that

$$\frac{\gamma^L}{\sqrt{3}} + \frac{2}{\sqrt{3}}\gamma^C\max(\Omega) = 1 \;\Leftrightarrow\; \gamma^C = \frac{\sqrt{3}-\gamma^L}{2\max(\Omega)}. \quad (32)$$

So, we have to choose φ so that $\max(\Omega)$ is minimal. This is the case if and only if

$$\varphi \in \{\pm\varphi_0 + m\omega_1 \;;\; m\in\mathbb{Z}\}, \quad (33)$$

where

$$\varphi_0 = \begin{cases}\omega_1/4-\pi/2 & \text{if } N_2 \text{ is odd}\\ \omega_1/2-\pi/2 & \text{if } N_2 \text{ is even}\end{cases}. \quad (34)$$

For such a φ, the value $\max(\Omega)$ is

$$\max(\Omega) = \sin(-\varphi_0) = \begin{cases}\cos(\omega_1/4) & \text{if } N_2 \text{ is odd}\\ \cos(\omega_1/2) & \text{if } N_2 \text{ is even}\end{cases}. \quad (35)$$

We note that the different values of φ in (33) either yield the same CFA as with φ_0, up to a displacement of the origin $\mathbf{cfa}[\mathbf{0}]$, or the CFA obtained after some permutation of its R,G,B channels. So we assume $\varphi=\varphi_0$ in the following.

Combining Eqns. (32), (35) and (31), Eqns. (15)-(17) can then be rewritten under the form given in Eqns. (18)-(22).

Acknowledgment

The author would like to thank K. Hirakawa at Harvard University for kindly providing a Matlab implementation of its demosaicking code as well as a preprint of its article [2] even before it was accepted for publication.

References

[1] K. Hirakawa and P. J. Wolfe, "Spatio-spectral color filter array design for enhanced image fidelity," in *Proc. of IEEE ICIP*, Sept. 2007.
[2] ——, "Spatio-spectral color filter array design for optimal image recovery," *IEEE Trans. Image Processing*, vol. 17, no. 10, pp. 1876–1890, Oct. 2008.
[3] ——, "A new spatio-spectral sampling paradigm for imaging and a novel color filter array design," U.S. Patent 067 472, June, 2008.
[4] K. Hirakawa and P. Wolfe, "Second-generation color filter array and demosaicking designs," in *Proc. of SPIE VCIP*, vol. 6822, 2008.
[5] B. K. Gunturk, J. Glotzbach, Y. Altunbasak, R. W. Schaffer, and R. M. Mersereau, "Demosaicking: Color filter array interpolation," *IEEE Signal Processing Mag.*, vol. 22, no. 1, pp. 44–54, Jan. 2005.
[6] K. Hirakawa and P. J. Wolfe, "Advancing the digital camera pipeline for mobile multimedia: Key challenges from a signal processing perspective," in *Proc. of IEEE ICASSP*, 5332–5335 2008.
[7] R. Lukac, B. Smolka, K. Martin, K. N. Plataniotis, and A. N. Venetsanopulos, "Vector filtering for color imaging," *IEEE Signal Processing Mag.*, vol. 22, no. 1, pp. 74–86, Jan. 2005.
[8] D. Alleyson, S. Susstrunk, and J. Herault, "Linear demosaicing inspired by the human visual system," *IEEE Trans. Image Processing*, vol. 14, no. 4, pp. 439–449, Apr. 2005.

[9] E. Dubois, "Frequency-domain methods for demosaicking of Bayer-sampled color images," *IEEE Signal Processing Lett.*, vol. 12, no. 12, pp. 847–850, Dec. 2005.
[10] B. E. Bayer, "Color imaging array," U.S. Patent 3 971 065, July, 1976.
[11] R. Lukac and K. N. Plataniotis, "Color filter arrays: Design and performance analysis," *IEEE Trans. Consumer Electron.*, vol. 51, no. 4, pp. 1260–1267, Nov. 2005.
[12] T. Kijima, H. Nakamura, J. T. Compton, J. F. Hamilton, and T. E. DeWeese, "Image sensor with improved light sensitivity," U.S. Patent 0 268 533, Nov., 2007.
[13] S. Yamanaka, "Solid state camera," U.S. Patent 4 054 906, Nov., 1977.
[14] M. Parmar and S. J. Reeves, "A perceptually based design methodology for color filter arrays," in *Proc. of IEEE ICASSP*, vol. 3, May 2004, pp. 473–476.
[15] W. Zhu, K. Parker, and M. A. Kriss, "Color filter arrays based on mutually exclusive blue noise patterns," *Journal of Visual Communication and Image Representation*, vol. 10, no. 3, pp. 245–267, Sept. 1999.
[16] A. Foi, M. Trimeche, V. Katkovnik, and K. Egiazarian, "Practical poissonian-gaussian noise modeling and fitting for single-image raw-data," *IEEE Trans. Image Processing*, vol. 17, no. 10, pp. 1737–1754, Oct. 2008.
[17] Y. Hel-Or, "The canonical correlations of color images and their use for demosaicing," HP Laboratories Israel, Tech. Rep. HPL-2003-164R1, Feb. 2004.
[18] J. Portilla, D. Otaduy, and C. Dorronsoro, "Low-complexity linear demosaicing using joint spatial-chromatic image statistics," in *Proc. of IEEE ICIP*, Sept. 2005.
[19] S. C. Pei and I. K. Tam, "Effective color interpolation in CCD color filter arrays using signal correlation," *IEEE Trans. Circuits Syst. Video Technol.*, vol. 13, pp. 503–513, 2003.
[20] B. A. Wandell, *Foundations of Vision*. Sinauer Associates, Inc., 1995.
[21] L. M. Hurvich and D. Jameson, "An opponent-process theory of color vision," *Psychological Review*, vol. 64, pp. 384–404, 1957.
[22] K. Hirakawa, "Cross-talk explained," in *Proc. of IEEE ICIP*, 2008, pp. 677–680.
[23] B. K. Gunturk, Y. Altunbasak, and R. M. Mersereau, "Color plane interpolation using alternating projections," *Proc. IEEE*, vol. 11, no. 9, pp. 997–1013, Sept. 2002.
[24] L. Nai-Xiang, C. Lanlan, T. Yap-Peng, and V. Zagorodnov, "Adaptive filtering for color filter array demosaicking," *IEEE Trans. Image Processing*, vol. 16, no. 10, pp. 2515–2525, Oct. 2007.
[25] D. Alleysson, L. Meylan, and S. Süsstrunk, "HDR CFA image rendering," in *Proc. of Eusipco*, Sept. 2006.